

6. L. Thevenaz, Slow and fast light in optical fibres, *Nat Photon* 2 (2008), 474–481.
7. V.M. Shalaev, Optical negative-index metamaterials, *Nat Photon* 1 (2007), 41–48.
8. K.L. Tsakmakidis, A.D. Boardman, and O. Hess, Trapped rainbow storage of light in metamaterials, *Nature* 450 (2007), 397–401.
9. J. He, Y. Jin, Z. Hong, and S. He, Slow light in a dielectric waveguide with negative-refractive-index photonic crystal cladding, *Opt Express* 16 (2008), 11077–11082.
10. W.T. Lu and S. Sridhar, Superlens imaging theory for anisotropic nanostructured metamaterials with broadband all-angle negative refraction, *Phys Rev B* 77 (2008), 233101.
11. D.R. Smith and D. Shurig, Electromagnetic wave propagation in media with indefinite permittivity and permeability tensors, *Phys Rev Lett* 90 (2003), 077405.
12. Y.J. Huang, W. T. Lu, and S. Sridhar, Nanowire waveguide made from extremely anisotropic metamaterials, *Phys Rev A* 77 (2008), 063836.
13. W.T. Lu and S. Sridhar, Slow light, open cavity formation, and large longitudinal electric field on slab waveguide made of indefinite metamaterials, arXiv, in press.
14. Q. Gan, Y.J. Ding, and F.J. Bartoli, Rainbow trapping and releasing at telecommunication wavelengths, *Phys Rev Lett* 102 (2009), 056801.
15. A. Reza, M.M. Dignam, and S. Hughes, Can light be stopped in realistic metamaterials? *Nature* 455 (2008), E10.
16. K.L. Tsakmakidis, A.D. Boardman, and O. Hess, Reply to can light be stopped in realistic metamaterials? *Nature* 450 (2008), E11.
17. W.T. Lu, Y.J. Huang, B.D.F. Casse, R.K. Banyal, and S. Sridhar, Storing light with single negative-index metamaterials, in press.
18. R.E. Collin, *Field theory of guided waves*, 2nd ed., IIE Press, New York, 1991.
19. V.G. Veselago, The electrodynamics of substances with simultaneously negative values of ϵ and μ , *Sov Phys Usp* 10 (1968), 509–518.
20. J.B. Pendry, A.J. Holden, D. Robbins, and W.J. Stewart, Magnetism from conductors and enhanced nonlinear phenomena, *IEEE Trans Microwave Theory Tech* 47 (1999), 2075–2084.
21. J.B. Pendry, A.J. Holden, W.J. Stewart, and I. Youngs, Extremely low frequency plasmons in metallic mesostructures, *Phys Rev Lett* 76 (1996), 4773–4776.
22. R. Shelby, D.R. Smith, and S. Schultz, Experimental verification of a negative index of refraction, *Science* 292 (2001), 77–79.
23. Q. Zhao, B. Du, L. Kang, H. Zhao, Q. Xie, B. Li, X. Zhang, J. Zhou, L. Li, and Y. Meng, Tunable negative permeability in an isotropic dielectric composite, *Appl Phys Lett* 92 (2008), 051106.
24. Q. Zhao, L. Kang, B. Du, H. Zhao, Q. Xie, X. Huang, B. Li, J. Zhou, and L. Li, Experimental demonstration of isotropic negative permeability in a three-dimensional dielectric composite, *Phys Rev Lett* 101 (2008), 027402.
25. L. Kang, Q. Zhao, H. Zhao, and J. Zhou, Magnetically tunable negative permeability metamaterial composed by split ring resonators and ferrite rods, *Opt Express* 16 (2008), 8825–8834.
26. D.R. Smith, S. Schultz, P. Markos, and C.M. Soukoulis, Determination of effective permittivity and permeability of metamaterials from reflection and transmission coefficients, *Phys Rev B* 65 (2002), 195104.
27. T. Koschny, P. Markos, D.R. Smith, and C.M. Soukoulis, Resonant and antiresonant frequency dependence of the effective parameters of metamaterials, *Phys Rev E* 68 (2003), 065602.
28. <http://www.ansoft.com/products/hf/hfss/>.
29. D. Schurig, J.J. Mock, B.J. Justice, S.A. Cummer, J.B. Pendry, A.F. Starr, D.R. Smith, Metamaterial electromagnetic cloak at microwave frequencies, *Science* 314 (2007), 977–980.
30. T.J. Yen, W.J. Padilla, N. Fang, D.C. Vier, D.R. Smith, J.B. Pendry, D.N. Basov, and X. Zhang, Terahertz magnetic response from artificial materials, *Science* 303 (2004), 1494–1496.
31. S. Linden, C. Enkrich, M. Wegener, J. Zhou, T. Koschny, and C.M. Soukoulis, Magnetic response of metamaterials at 100 terahertz, *Science* 306 (2004), 1351–1353.
32. H.-T. Chen, J. F. O'Hara, A. K. Azad, and A. J. Taylor, R.D. Averitt, D. Shrekenhamer, and W. J. Padilla, Experimental demonstration of frequency-agile terahertz metamaterials, *Nat Photon* 2 (2008), 295–298.

© 2009 Wiley Periodicals, Inc.

TRANSFORMATION OPTICS-INSPIRED METAMATERIAL COATINGS FOR CONTROLLING THE SCATTERING RESPONSE OF WEDGE/CORNER-TYPE STRUCTURES

Ilaria Gallina,^{1,2} Giuseppe Castaldi,¹ and Vincenzo Galdi¹

¹ Waves Group, Department of Engineering, University of Sannio, Benevento, Italy; Corresponding author: vgaldi@unisannio.it

² Department of Environmental Engineering and Physics, University of Basilicata, Potenza, Italy

Received 20 May 2009

ABSTRACT: Transformation optics has recently emerged as a powerful and systematic approach to design application-oriented metamaterials. In this letter, following up on our previous studies on thin planar retroreflectors, we show how it is possible, in principle, to design “transformation medium” coatings capable of controlling the scattering response of metallic corner- and wedge-type structures so as, e.g., to strongly enhance the specularly reflected component. We validate our results via a full-wave study of the near- and far-field responses, and envisage possible applications. © 2009 Wiley Periodicals, Inc. *Microwave Opt Technol Lett* 51: 2709–2712, 2009; Published online in Wiley InterScience (www.interscience.wiley.com). DOI 10.1002/mop.24720

Key words: transformation optics; metamaterials; scattering

1. INTRODUCTION

The rapid advances in the engineering of metamaterials with controllable anisotropy and spatial inhomogeneity have recently led to the development of a novel framework, typically referred to as “transformation optics” [1, 2], for the design of metamaterial-based devices that allow unprecedented control in the electromagnetic (EM) response. Besides the celebrated “invisibility cloaking” (experimentally verified at microwave frequencies [3] and within the visible range [4]), many other exciting developments are foreseen in a wide range of applications (see, e.g., [5–13] for a sparse sampling).

In a series of ongoing investigations, we have been concerned with the application of transformation optics to the design of coatings for controlling the scattering response of flat metallic structures. For instance, in [14], we addressed the design of thin planar retroreflectors inspired by the dihedral corner-reflector geometry. In this framework, we showed that it was possible to design a metamaterial layer (with anisotropic and inhomogeneous distribution, and with constitutive parameters values that were positive, everywhere limited, and not particularly high), which laid on a metallic plate, would lead to a strong enhancement of the monostatic radar cross-section (RCS) response.

Following up on the earlier study, in this letter, we deal with more complicate geometries featuring wedge- or corner-type metallic scatterers. To illustrate the potentials of the transformation-optics approach in controlling the scattering response, we focus on a rather challenging example, namely, the design of metamaterial coatings capable of inducing an overall behavior similar to that exhibited by a planar metallic sheet (i.e., with a predominant specular response). Such response may be very useful in radar countermeasure applications, where dealing with wedge/corner-type structures represents a critical issue for the reduction of the overall visibility.

Following the standard transformation-optics approach, we first design the desired field behavior, for both the wedge- and corner-

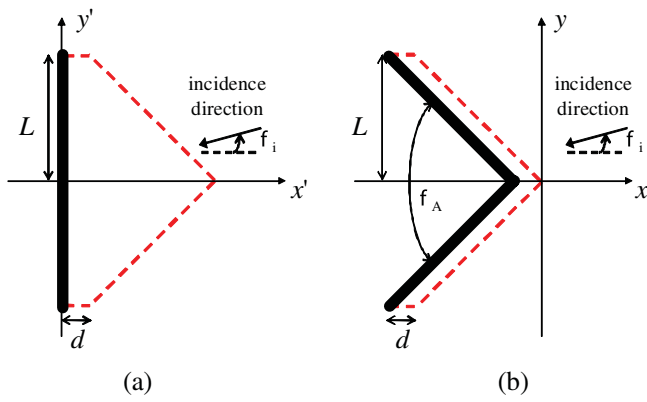


Figure 1 Problem geometry. (a) Planar metallic reflector in the (x', y') space. (b) Proposed wedge-type reflector in the transformed (x, y) space. Black thick lines denote the PEC boundaries; red dashed lines delimit the free-space (a) and coating (b) regions involved in the transformation. [Color figure can be viewed in the online issue, which is available at www.interscience.wiley.com]

type scatterers, in a fictitious space characterized by a suitable “flattening” metric. Next, in view of the formal invariance of Maxwell’s equations under coordinate transformations, we translate such a behavior in a conventional flat, Cartesian space filled by a suitable (anisotropic and spatially inhomogeneous) “transformation medium.”

Accordingly, the rest of this letter is organized as follows. In Section 2, we illustrate the problem geometry and parameters. In Section 3, we present a number of representative results, pertaining to the near- and far-field responses. Finally, in Section 4, we provide some conclusions and hints for future research.

2. GEOMETRY AND PARAMETERS

The configurations of interest for our two-dimensional (2D) prototype study are illustrated in Figures 1 and 2. In both cases [cf. Figs. 1(a) and 2(a)], we start from a fictitious (x', y', z') space featuring the desired response (i.e., mainly specular reflection), which is most easily achievable considering an infinitely long (in the z -direction) perfectly electric conducting (PEC) sheet (black thick line) of width $2L$ in free space. To induce such a behavior in the wedge-type [cf. Fig. 1(b)] and corner-type [cf. Fig. 2(b)] PEC configurations of interest in the actual (x, y, z) physical space, we need to find two coordinate transformations capable of mapping the PEC planar sheet in the fictitious space onto such configurations. For the wedge case, a simple transformation is given by

$$x = \frac{x'd}{d + a(|y'| - L)} - d + a|y'|, y = y', z = z', |y'| \leq L, \quad (1)$$

where the parameter a is related to the wedge aperture angle ϕ_A [see Fig. 1(b)] via $a = -\cot(\phi_A/2)$, whereas the parameter d controls the aspect-ratio of the transformed geometry. Although such a transformation could, in principle, still be applicable to corner-type geometries [considering aperture angles $\phi_A > 180^\circ$ in Fig. 1(b)], for reasons that will become clear hereafter, it is expedient to deal with the corner-case using a different transformation:

$$x = \frac{x'd}{a(|y'| - L)} - aL - d + a|y'|, y = y', z = z', |y'| \leq L, \quad (2)$$

where the parameter a is now related to the corner aperture angle ϕ_A [see Fig. 2(b)] via $a = \cot(\phi_A/2)$. Note that for square (i.e., $\phi_A = 90^\circ$) wedges and corners, we have $a = -1$ and $a = 1$, respectively, and that for $\phi_A = 180^\circ$ (i.e., already flat geometries) we have $a = 0$, and the transformations reduce to rigid translations along the x axis. The mapping, via (1) and (2), of the planar surface plus a portion of free-space [bounded by the red dashed lines in Figs. 1(a) and 2(a)] in the fictitious (x', y', z') space onto a wedge/corner-shaped configurations in the transformed space (x, y, z) is illustrated in Figures 1(b) and 2(b), respectively; PEC sheets forming the wedge/corner (black thick lines) have width $L\sqrt{a^2 + 1}$ (i.e., the structures have a total aperture of $2L$), and are topped by a slab of thickness d (red dashed lines). Following Refs. [1, 2], the same behavior can be obtained in a conventional, flat Cartesian space, provided that the slabs in the transformed regions are filled up by “transformation media” with relative permittivity and permeability tensors given by

$$\epsilon_r = \mu_r = J \cdot J^T [\det(J)]^{-1}, \quad (3)$$

where $J = \partial(x, y, z)/\partial(x', y', z')$ is the Jacobian matrix of the transformations in (1) and (2), and the superfix T denotes transposition. As a result, we obtain the following explicit expressions, for the wedge- and corner-type scatterers, respectively,

$$\epsilon_r(x, y) = \mu_r(x, y) = \begin{bmatrix} \frac{a^2 g_w^2(x, y) + d^2}{d(d + a|y| - aL)} & -\frac{a}{d} \text{sgn}(y) g_w(x, y) & 0 \\ -\frac{a}{d} \text{sgn}(y) g_w(x, y) & 1 + \frac{a}{d}(|y| - L) & 0 \\ 0 & 0 & 1 + \frac{a}{d}(|y| - L) \end{bmatrix}, \quad (4)$$

$$\epsilon_r(x, y) = \mu_r(x, y) = \begin{bmatrix} \frac{a^2 g_c^2(x, y) + d^2}{da(|y| - L)} & -\frac{a}{d} \text{sgn}(y) g_c(x, y) & 0 \\ -\frac{a}{d} \text{sgn}(y) g_c(x, y) & \frac{a}{d}(|y| - L) & 0 \\ 0 & 0 & \frac{a}{d}(|y| - L) \end{bmatrix}, \quad (5)$$

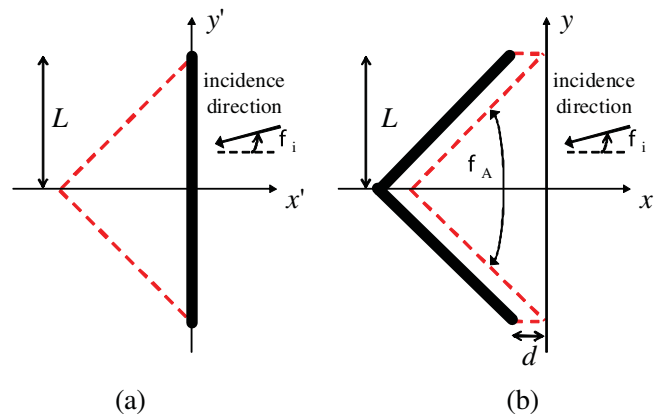


Figure 2 As in Figure 1, but for the corner case. [Color figure can be viewed in the online issue, which is available at www.interscience.wiley.com]

where $g_w(x,y) = x - 2a|y| + aL$, $g_c(x,y) = x - 2a|y| + L + aL + d$, $\text{sgn}(\cdot)$ denotes the signum function, and the anisotropy and spatial inhomogeneity are evident. Note that the coordinate transformations in (1) and (2) ensure perfect-impedance matching (i.e., zero reflection) at the interface with free-space.

As in Ref. [14], the properties of the above transformation media can be better understood diagonalizing the tensors in (4) and (5). One can show that, in both cases, the material parameter distributions and the principal axes exhibit mirror symmetry (inherited from the original planar configuration) around the x -axis. Moreover, as for the retrodirective-reflector case in Ref. [14], the constitutive parameter values for the wedge coating turn out to be all positive, everywhere limited, and not particularly high, thereby not implying insurmountable technological challenges in their fabrication. As an example, for a coating thickness $d = L/(3\sqrt{2})$, the variation ranges for the components along the local eigenvector directions in the x - y plane and along the z -direction are [0.10, 0.95], [1.05, 10.5], and [1.03, 5.23], respectively. On the other hand, the constitutive parameters associated with the corner coating are *negative*, and one of them can be locally divergent. This is not surprising, in view of the *space-folding* properties of the transformation (also observed, e.g., in anti-cloak-type configurations [12, 13]), but renders the fabrication of the corresponding transformation media practically unfeasible within the current technological capabilities. We decided nevertheless to study this configuration too, since the potentially interesting properties exhibited may serve as a further motivation (together, e.g., with the anti-cloak-type configurations [12, 13]) for advances in the synthesis of double-negative metamaterials with extreme parameter values. In this connection, we also point out that the transformation in (1), though technically applicable to the corner case as well (using values of the aperture angle $\phi_A > 180^\circ$), would lead to a combination of double-positive and double-negative media with extreme parameters, which would likely cause convergence problems in the numerical simulations (see Section 3 later). This is the reason why we chose the transformation in (2).

3. REPRESENTATIVE RESULTS

As in Ref. [14], we carried out a study of the near- and far-field responses of the wedge- and corner-type configurations, based on finite-element method (FEM) full-wave simulations [15]. We considered a time-harmonic $[\exp(j\omega t)]$ plane-wave excitation with unit-amplitude z -directed electric field and incidence angle ϕ_i , and a computational domain of sidelength $14\lambda_0$ (λ_0 being the free-space wavelength), discretized into $\sim 800,000$ unknowns. In what follows, for brevity, attention will be focused on the representative cases of square ($\phi_A = 90^\circ$) wedges and corners.

Some representative near-field maps, for oblique incidence with $\phi_i = 15^\circ$, are shown in Figure 3, for the configurations under examination: plain PEC [Fig. 3(a)] and metamaterial-coated wedges [Fig. 3(b)], plain PEC [Fig. 3(c)] and metamaterial-coated corners [Fig. 3(d)], and plain PEC sheet [Fig. 3(e)], with moderate electrical apertures and coating thicknesses. The specular responses of the proposed metamaterial-coated configurations in Figures 3(b) and 3(d) are clearly visible from the wavefront shapes, remarkably different from the uncoated cases in Figures 3(a) and 3(c), and in complete agreement with that observed in the plain PEC sheet reference case [Fig. 3(e)]. In order to obtain a clear visualization of the field inside the structures, we chose a moderate thickness value $d = L/(3\sqrt{2}) = \lambda_0$. However, consistently similar behaviors were observed for thinner slabs.

Subsequently, we calculated the 2D *bistatic* RCS [16] $\sigma_{2D}(\phi)$, with $\phi = \arctan(y/x)$, constructing a Bessel-Fourier expansion of

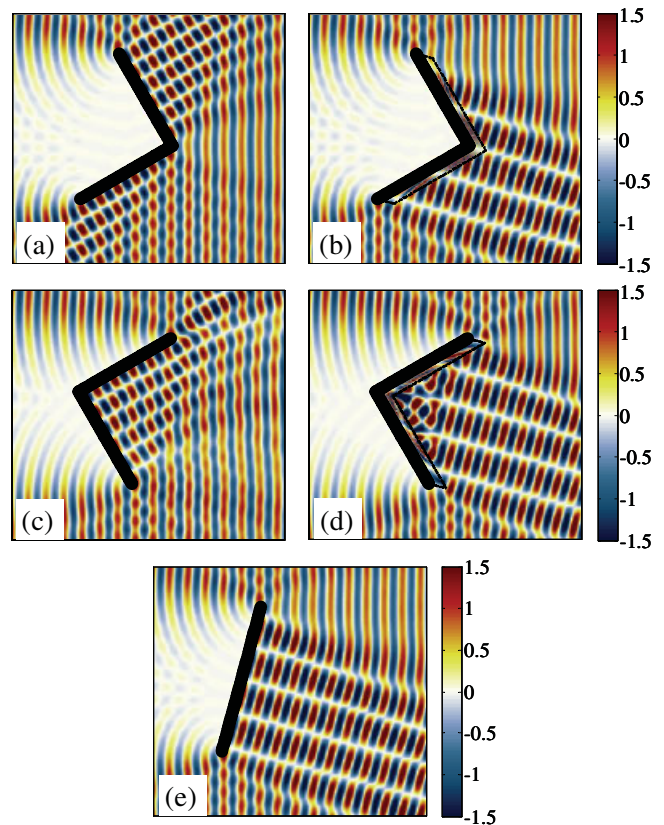


Figure 3 FEM-computed near-field maps (real part of electric field) for unit-amplitude plane-wave oblique ($\phi_i = 15^\circ$) incidence. (a), (b) Plain PEC and metamaterial-coated square ($\phi_A = 90^\circ$) wedges, respectively, with $2L = 6\sqrt{2}\lambda_0$ and $d = \lambda_0$. (c), (d) Plain PEC and metamaterial-coated square corners, with same parameters. (e) Plain PEC sheet. For computational convenience, the structures are rotated and the illuminating wave is impinging horizontally (from right). [Color figure can be viewed in the online issue, which is available at www.interscience.wiley.com]

the scattered electric field via point-matching of the FEM solution on a near-zone circle. The behavior observed in the near field maps is confirmed by the bistatic RCS responses, as shown in Figures 4 and 5, for a reduced coating thickness $d = L/(6\sqrt{2}) = \lambda_0/2$. Besides the obvious forward-direction peak, the two uncoated structures exhibit the well-known scattering features (displayed as blue-dotted curves). Specifically, the wedge structure (see Fig. 4) exhibits two lobes (asymmetrical, in view of the oblique incidence) at direction $90^\circ - \phi_i$ and $270^\circ - \phi_i$, arising from the single reflections at each face, whereas the corner structure (see Fig. 5) exhibits a strong retroreflection peak arising from the double reflection at its faces. These features are suppressed in the metamaterial-coated structures, and a strong specular ($\phi = -\phi_i$) peak is instead observed (black-solid curves), practically indistinguishable (on the plot scale) from the plain PEC sheet reference case (red-dashed curves).

Finally, Figure 6 compares the responses of the two proposed metamaterial-coated structures to that of the reference plain PEC sheet in terms of the *specular* RCS (i.e., the value of the bistatic RCS, normalized to the free-space wavelength, for $\phi = -\phi_i$), as a function of the incidence angle. Once again, very similar behaviors are observed for the three configurations.

It is worth noting that the above responses pertain to ideal (lossless) metamaterials. However, as in Ref. [14], they were found to be not dramatically affected by the presence of small losses.

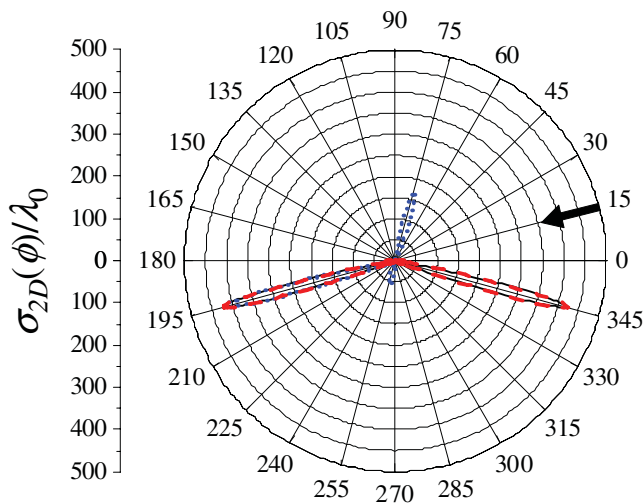


Figure 4 As in Figure 3, but 2D bistatic RCS (scaled to the free-space wavelength), for plain PEC wedge (blue-dotted curve) and planar sheet (red-dashed curve), and for metamaterial-coated wedge (black-solid curve) with $d = \lambda_0/2$. The coated-wedge and planar-sheet responses are practically indistinguishable on the scale of the plot. The incidence direction is marked by a thick arrow. [Color figure can be viewed in the online issue, which is available at www.interscience.wiley.com]

4. CONCLUSIONS

In this letter, we have addressed the design of metamaterial coatings capable of controlling the scattering response of wedge- and corner-type metallic structures. In particular, following the transformation optics approach, we have derived the constitutive properties of anisotropic and spatially inhomogeneous “transformation-medium” coatings, which laid on a wedge/corner metallic scatterer, exhibit the specular response typical of a standard planar metallic reflector. These coatings could find interesting applications in radar countermeasure applications, where the presence of wedges and corners represents a critical problem.

Current and future studies are aimed at exploring the technological viability of the proposed coatings, via simplified implementations (featuring, e.g., reduced parametric ranges, single-negative, and/or nonmagnetic materials).

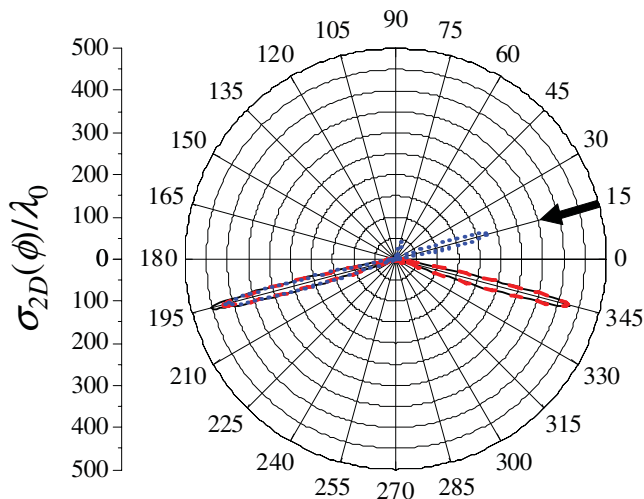


Figure 5 As in Figure 4, but for plain PEC (blue-dotted curve) and metamaterial-coated (black-solid curve) corner. [Color figure can be viewed in the online issue, which is available at www.interscience.wiley.com]

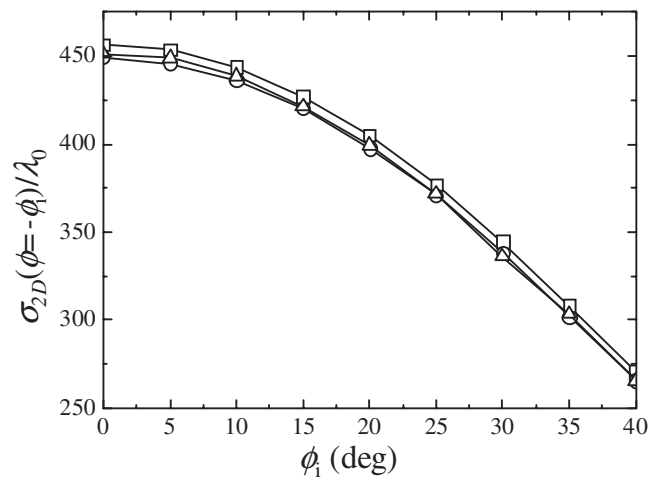


Figure 6 As in Figures 4 and 5, but specular ($\phi = -\phi_1$) RCS as a function of the incidence angle ϕ_1 , for metamaterial-coated wedge and corner, and for plain PEC sheet (circles, squares, and triangles, respectively)

ACKNOWLEDGMENT

The kind assistance of Dr. Bruno Bisceglia (University of Salerno, Italy) in the full-wave simulations is gratefully acknowledged.

REFERENCES

1. D. Schurig, J. B. Pendry, and D. R. Smith, Calculation of material properties and ray tracing in transformation media, *Opt Express* 14 (2006), 9794–9804.
2. U. Leonhardt and T. G. Philbin, General relativity in electrical engineering, *New J Phys* 8 (2006), 247.
3. D. Schurig, J. J. Mock, B. J. Justice, S. A. Cummer, J. B. Pendry, A. F. Starr, and D. R. Smith, Metamaterial electromagnetic cloak at microwave frequencies, *Science* 314 (2006), 977–980.
4. I. I. Smolyaninov, Y. J. Hung, and C. C. Davis, Two-dimensional metamaterial structure exhibiting reduced visibility at 500 nm, *Opt Lett* 33 (2008), 1342–1344.
5. A. Greenleaf, Y. Kurylev, M. Lassas, and G. Uhlmann, Electromagnetic wormholes and virtual magnetic monopoles from metamaterials, *Phys Rev Lett* 99 (2007), 183901.
6. H. Y. Chen and C. T. Chan, Transformation media that rotate electromagnetic fields, *Appl Phys Lett* 90 (2007), 241105.
7. F. Kong, B.-I. Wu, J. A. Kong, J. Huangfu, S. Xi, and H. Chen, Planar focusing antenna design by using coordinate transformation technology, *Appl Phys Lett* 91 (2007), 253509.
8. B. Donderici and F. L. Teixeira, Metamaterial blueprints for reflectionless waveguide bends, *IEEE Microwave Wireless Compon Lett* 18 (2008), 233–235.
9. A. V. Kildishev and E. E. Narimanov, Impedance-matched hyperlens, *Opt Lett* 32 (2007), 3432–3434.
10. M. Tsang and D. Psaltis, Magnifying perfect lens and superlens design by coordinate transformation, *Phys Rev B* 77 (2008), 035122.
11. J. Li and J. B. Pendry, Hiding under the carpet: a new strategy for cloaking, *Phys Rev Lett* 101 (2008), 203901.
12. H. Chen, X. Luo, H. Ma, and C.T. Chan, The anti-cloak, *Opt Express* 16 (2008), 14603–14608.
13. G. Castaldi, I. Gallina, V. Galdi, A. Alù, and N. Engheta, Cloak/anti-cloak interactions, *Opt Express* 17 (2009), 3101–3114.
14. I. Gallina, G. Castaldi, and V. Galdi, Transformation media for thin planar retrodirective reflectors, *IEEE Antennas Wireless Propagat Lett* 7 (2008), 603–605.
15. COMSOL MULTIPHYSICS—User’s Guide. COMSOL AB, 2005.
16. E. F. Knott, J. F. Shaeffer, and M. T. Tuley, Radar cross section, 2nd ed., Artech House, London, 1993.